

Solamargine inhibits gastric cancer progression via inactivation of STAT3/PD-L1 signaling

XIONGXIANG LIU, LIN SONG, WEN LIU, BIN LIU, LANG LIU and YAO SU

Department of Gastroenterology, Xiangtan Central Hospital, Xiangtan, Hunan 411100, P.R. China

Received February 6, 2024; Accepted September 2, 2024

DOI: 10.3892/mmr.2024.13400

Abstract. Gastric cancer (GC) is characterized by a high mortality rate (70%) worldwide. Programmed cell death-1 and its ligand, programmed cell death ligand 1 (PD-L1), are vital immune checkpoints, which serve a notable role in GC. Solamargine, an extract from traditional Chinese medicine Long Kui, exerts suppressive effects on several types of cancer including cervical, lung and prostate cancer. However, the association between solamargine and PD-L1 in GC remains unclear. Therefore, the present study aimed to investigate the underlying mechanism of solamargine on GC. Specifically, 5-ethynyl-2'-deoxyuridine and Transwell assays were performed to assess GC cell proliferation, invasion and migration. Additionally, GC cells (HGC-827 and NCI-N87) were stimulated with 20 ng/ml recombinant human IL-6 for 24 h, before the protein expression levels of PD-L1 were measured using western blot analysis. Furthermore, T cell function was evaluated through incubation of Jurkat T cells with solamargine. The results demonstrated that solamargine could markedly inhibit GC cell proliferation, migration and invasion, by inhibiting STAT3 signaling. In addition, GC cell treatment with solamargine downregulated the expression of PD-L1. Furthermore, solamargine reversed the IL-6-induced PD-L1 upregulation in GC cells by downregulating STAT3 activity. Additionally, the results demonstrated that solamargine inhibited IL-6-induced PD-L1 upregulation of GC cells. This suggests that solamargine exerted an immunostimulatory activity in GC. In conclusion, the present study indicated that solamargine may inhibit the progression of GC by suppressing STAT3/PD-L1 signaling. Therefore, treatment with solamargine may serve as novel strategy for the treatment of GC.

Introduction

Gastric cancer (GC) is the fifth highest cause of tumor-associated mortalities worldwide (1). At present, the most common treatment strategies for GC includes chemotherapy, surgery, radiation, immunotherapy and target treatment such as trastuzumab (2). Despite advancements, the overall 5-year survival rate of patients with advanced GC remains <30% (3,4), therefore exploring the novel and effective strategies for the treatment of GC is required.

Recently, traditional Chinese medicines have been garnering attention as a prospect of tumor treatments due to their immune-regulation functions, multiple targets and fewer side effects (5). The traditional Chinese herb, Long Kui (*Solanum nigrum* Linn), contains a number of steroidal alkaloids and has been reported to exert various bioactive effects, including antitumor and anti-inflammatory properties (6,7). In particular, solamargine is an extract from Long Kui that has been reported to confer antitumor properties in several types of cancer, including cervical, lung and prostate cancer, in addition to antiviral and anti-inflammatory properties (7-10). However, to the best of our knowledge, the molecular mechanism underlying the antitumor effects of solamargine has not yet been elucidated.

T cell immunity serves a role in maintaining body homeostasis by selectively eliminating pathogens and abnormal cells (10). However, the uncontrolled hyperactivation of T cells due to immune system disorder can destroy normal cells (11). A previous study reported that programmed cell death-1 (PD-1) and programmed cell death ligand 1 (PD-L1) can maintain the regulation of T cell activities under normal conditions, thereby preventing the development of autoimmune reactions (12). Furthermore, STAT3 is a modulator in cancer and inflammatory responses (13,14). It has been previously reported that STAT3 activation can promote the progression of numerous types of cancer, including GC, ovarian cancer and breast cancer (15,16). In addition, other studies have demonstrated that STAT3 can promote tumorigenesis by activating PD-L1 (17,18). Cancer cells highly expressed PD-L1 and leading to T cell exhaust, which has been documented to be responsible for cancer immune escape, which impacts the efficacy of cancer therapy (19). However, to the best of our knowledge, the possible association between solamargine and PD-L1/STAT3 signaling remains to be elucidated. Therefore, the present study

Correspondence to: Dr Xiongxiang Liu, Department of Gastroenterology, Xiangtan Central Hospital, 120 Heping Road, Xiangtan, Hunan 411100, P.R. China
E-mail: xiongxiangliu12@126.com

Key words: STAT3, programmed cell death ligand 1, solamargine

aimed to evaluate the mechanism underlying the effect of solamargine on GC.

Material and methods

Cell culture. GC cell lines, NCI-N87 and HGC-27, and Jurkat T cells were purchased from the American Type Culture Collection. Cells were cultured in RPMI 1640 medium (Gibco; Thermo Fisher Scientific, Inc.) supplemented with 10% FBS (Gibco; Thermo Fisher Scientific, Inc.), 100 µg/ml streptomycin and 100 µg/ml penicillin, in an incubator with 5% CO₂ at 37°C. To evaluate the effect of solamargine (MedChemExpress) on GC cells, GC cells were induced with 20 ng/ml IL-6 (MilliporeSigma) for 24 h at 37°C, and then treated with 10 µM solamargine for 48 h at 37°C.

Cell Counting Kit-8 (CCK-8) assay. For CCK-8 assays, a total of 5x10³ HGC-27 or NCI-N87 cells were seeded in culture plates and incubated at 37°C overnight. Following treatment with 5, 10 or 20 µM solamargine at 37°C for 48 h, cells were then incubated with 10 µl CCK-8 reagent (Beyotime Institute of Biotechnology) at room-temperature for 4 h. Subsequently, the absorbance of each well was measured at OD450 using a plate microreader (Thermo Fisher Scientific, Inc.).

Transwell assay. A total of 5x10⁴ HGC-27 or NCI-N87 cells were seeded into the upper chamber (serum-free RPMI 1640 medium) of the Transwell insert (3 µm, cat. no. 3414; Corning, Inc.). For the invasion assay, the upper chamber was precoated with 50 µl Matrigel for 3 h at 37°C. As for the migration assay, the upper chamber was not precoated with Matrigel. Following incubation for 12 h at 37°C, cells in the upper chamber were removed and those in the lower chamber (10% FBS RPMI 1640 medium) were fixed with 100% anhydrous ethanol for 30 min at room temperature, followed by staining with 1% crystal violet for 1 h at room temperature. The cells were then counted under an inverted light microscope (Leica Microsystems GmbH).

5-Ethynyl-2'-deoxyuridine (EdU) assay. Following incubation overnight at 37°C, HGC-27 or NCI-N87 cells at a density of 4x10⁴ were treated with 50 µM EdU solution (cat. no. C10338; Thermo Fisher Scientific, Inc.) for 4 h at 37°C. Subsequently, cells were fixed with 4% formaldehyde for 24 h at room temperature, followed by permeabilization for 10 min in 0.5% Triton X-100. Cells were then incubated with 100 µl Apollo reaction cocktail (Guangzhou RiboBio Co., Ltd) for 30 min at room temperature and DNA was stained with 100 µl/well DAPI (Wuhan Servicebio Technology Co., Ltd.) for 30 min at room temperature. The stained cells were observed using a fluorescence microscope (magnification, x100). A total of three random fields were selected and the Edu-positive cells were counted.

Immunofluorescence staining. GC cells were seeded in 24-well plates. After treatments with 5 or 10 µM solamargine for 48 h at 37°C, cells were fixed with 4% paraformaldehyde at room temperature for 15 min and permeabilized with 0.5% Triton X-100 for 2 min at room temperature. After blocking with 5% BSA (MilliporeSigma) for 2 h at room temperature, the

cells were then incubated with antibodies against phosphorylated (p)-STAT3 (1:200; cat. no. ab267373; Abcam), STAT3 (1:200; cat. no. ab68153; Abcam), cleaved caspase 3 (1:200; cat. no. ab32042; Abcam) or caspase 3 (1:200; cat. no. ab32351; Abcam) at 4°C overnight. Subsequently, cells were incubated with the goat anti-rabbit IgG (conjugated to Alexa Fluor® 594) secondary antibody (1:500; cat. no. ab150080; Abcam) for 1 h at room temperature. The GC cells were stained with 500 µl DAPI for 10 min at room temperature. Finally, images of the stained cells were captured using a confocal microscope (Carl Zeiss AG).

Western blotting. Total protein was extracted from HGC-27 and NCI-N87 cells using RIPA buffer (Beyotime Institute of Biotechnology) and protein concentration was quantified using a BCA kit (Beyotime Institute of Biotechnology). Subsequently, total proteins (20 µg/lane) were separated using SDS-PAGE on a 10% gel and transferred onto PVDF membranes. Following blocking with 5% non-fat milk at room temperature for 1 h, the membranes were incubated with primary antibodies against PD-L1 (1:1,000; Abcam; cat. no. ab228415), c-Myc (1:1,000; Abcam; cat. no. ab32072) and β-actin (1:1,000; Abcam; cat. no. ab8227) overnight at 4°C. Subsequently, the membranes were incubated with the corresponding secondary goat anti-rabbit antibody (1:5,000; cat. no. ab288151; Abcam) at room temperature for 1 h. After which, the targeted proteins were visualized using with ECL kit (Beyotime Institute of Biotechnology). The Odyssey Imaging System (LI-COR Bio) was used to scan membranes and the data were analyzed using Odyssey version 2.0 software (LI-COR Bio).

TUNEL staining assay. HGC-27 or NCI-N87 cells were seeded into 24-well plates. After treatments with 5 or 10 µM solamargine for 48 h at 37°C, cells were fixed with 4% paraformaldehyde at room temperature for 15 min, before being permeabilized with 0.5% Triton X-100 for 2 min at room temperature. Subsequently, apoptotic cells were stained for 1 h at 37°C using the One Step TUNEL Apoptosis Assay kit (Beyotime Institute of Biotechnology). Cell nuclei were stained with 100 µl/well DAPI (10 µg/ml; Wuhan Servicebio Technology Co., Ltd.) for 30 min at room temperature. Finally, images of the positive apoptotic cells in three random fields were captured using a confocal microscope (Carl Zeiss AG).

Flow cytometry analysis. Jurkat cells were stimulated with anti-CD3/CD28 antibodies (1:100; Thermo Fisher Scientific, Inc.; cat. no. 11161D) for 24 h at 37°C and then co-cultured with NCI-N87 or HGC-27 cells pretreated with 10 µM solamargine for 48 h at 37°C. To isolate the Jurkat cells, 5x10⁵ cells were centrifuged for 2 min at 500 x g at 4°C and incubated with APC anti-CD69 (dilution 1:100; Biolegend; cat. no. 985206) for 30 min at room temperature in the dark, followed washing with PBS for three times and centrifugation at 500 x g for 2 min at 4°C. The stained cells (HGC-27 or NCI-N87 cells) were analyzed using flow cytometry (BD Biosciences). FlowJo (version 10.0.7; FlowJo LLC) software was used for data analysis.

Statistical analysis. All data are expressed as the mean ± standard deviation. The results were analyzed using GraphPad

Prism (version 7.0; Dotmatics). The differences between two groups were assessed using an unpaired Student's t-test, whilst those among multiple groups were compared using one-way ANOVA, followed by Tukey's post hoc test. $P < 0.05$ was considered to indicate a statistically significant difference.

Results

Solamargine reduces the proliferation ability of GC cells. To investigate the effect of solamargine on GC, GC cells were treated with 5, 10 or 20 μM solamargine for 48 h. It was demonstrated that solamargine decreased the viability of NCI-N87 (Fig. 1A) and HGC-27 cells (Fig. 1B), with all concentrations of solamargine significantly reducing the cell viability compared with that in the control group. In addition, the percentage of EdU-positive HGC-27 (Fig. 1C) and NCI-N87 cells (Fig. 1D) was found to be significantly decreased after treatment with 5 and 10 μM solamargine compared with that in the control group. These results suggest that solamargine can significantly attenuate the viability and proliferation of GC cells.

Solamargine reduces the migration and invasion of GC cells. Subsequently, to evaluate the effect of solamargine on the migration and invasion of GC cells, Transwell assays were performed. The results indicated that the migration of NCI-N87 and HGC-27 cells were significantly decreased by 5 and 10 μM solamargine compared with that in the control group (Fig. 2A). Furthermore, the invasion of NCI-N87 and HGC-27 cells were also significantly reduced by 5 and 10 μM solamargine compared with that in the control group (Fig. 2B). Taken together, the aforementioned findings suggest that solamargine can reduce the migration and invasion of GC cells.

Solamargine promotes the apoptosis of GC cells through the caspase 3 pathway. To assess the effect of solamargine on GC cell apoptosis, a TUNEL staining assay was next performed. Subsequently, 5 and 10 μM solamargine was found to significantly increase the percentage of TUNEL-positive NCI-N87 and HGC-27 cells compared with that in the control group (Fig. 3A). Furthermore, the relative fluorescence intensity of cleaved caspase 3 was significantly increased in 5 and 10 μM solamargine-treated NCI-N87 and HGC-27 cells (Fig. 3B). This suggests that solamargine notably induced GC cell apoptosis through the caspase-3 signaling pathway, which was demonstrated by the relative increase in fluorescence intensity of cleaved caspase 3.

Solamargine reverses the IL-6-induced activation of STAT3/PD-L1 signaling. To assess the effect of solamargine on STAT3/PD-L1 signaling, GC cells were treated with IL-6 before the expression levels of PD-L1 and c-Myc were investigated using western blotting. It was demonstrated that IL-6 significantly increased the protein levels of PD-L1 and c-Myc in HGC-27 (Fig. 4A) and NCI-N87 cells (Fig. 4B) compared with that in the control group. However, treatment with IL-6 and 5 or 10 μM solamargine significantly reversed this increased protein expression levels of PD-L1 and c-Myc in HGC-27 (Fig. 4A) and NCI-N87 cells (Fig. 4B) compared with those in the IL-6 treatment alone. Additionally, the IL-6-induced upregulation of STAT3 phosphorylation in HGC-27 (Fig. 4C)

and NCI-N87 cells (Fig. 4D) was reversed by 5 and 10 μM solamargine treatment compared with that in the IL-6 treatment alone group. This data suggest that solamargine can reverse the IL-6-induced activation of STAT3/PD-L1 signaling.

Solamargine activation of T cells. A previous study reported that PD-L1 upregulation can promote the escape of tumor cells from the attack of T cells (20). Furthermore, the aforementioned results of the present study demonstrated that solamargine can reduce the protein expression levels of PD-L1. Therefore, to investigate the effect of solamargine on T cells, Jurkat T cells were stimulated with anti-CD3/CD28 antibodies. Subsequently, Jurkat T cells were co-cultured with non-treated or solamargine-treated NCI-N87 or HGC-27 cells. The results demonstrated that solamargine could increase the expression of CD69 (T cell activation marker) in Jurkat T cells (Fig. 5A and B). In summary, solamargine may activate T cells.

Discussion

The incidence of GC worldwide had increased by ~75% in 2023 (21). Therefore, the pathogenic mechanism of GC should be determined. In the present study, the results demonstrated that solamargine can reduce the migration and invasion of GC cells. In addition, solamargine was found to reverse the IL-6-induced PD-L1 and STAT3 phosphorylation upregulation in GC cells, in addition to promoted T cell activation. To the best of our knowledge, the present study was the first to investigate the association between solamargine and T cell activation. The results of the present study suggest that solamargine may serve as a novel therapeutic agent in GC by activation of T cells.

PD-L1 serves a role in immunotherapy, since PD-L1 down-regulation enables T cells to recognize tumor cells (22,23). The results of the present study demonstrated that solamargine reduced the proliferation of GC cells and reduced the protein expression levels of PD-L1. Traditional Chinese medicine monomers have been previously documented to complement the efficacy of immunotherapy for the treatment of malignant tumors. A previous study by Yu *et al* (24) demonstrated that the traditional Chinese medicine monomer aianthone can improve the therapeutic efficacy of anti-PD-L1 mAb (Bio X Cell) in melanoma cells by inhibiting the c-Jun signaling pathway. Additionally, another study by Liu *et al* (25) previously revealed that berberine can reduce PD-L1 expression levels in non-small cell lung cancer cells and promote anti-tumor immunity, thus inhibiting the deubiquitination activity of CSN5 and served as an immune checkpoint inhibitor. Therefore, the anti-PD-L1 potential of monomers in GC cancer treatment should be further investigated.

The results of the present study also suggested that solamargine reduced the levels of STAT3 in GC cells. Emerging evidence suggests that STAT3 activation can promote tumorigenesis in several types of cancer, including GC (26-28). Therefore, it was hypothesized that solamargine can inhibit the tumorigenesis of GC by inactivating the STAT3 signaling pathway. Furthermore, PD-L1 has been previously shown to be positively regulated by STAT3 during cancer progression. Jiang *et al* (29) previously found that tripartite motif-containing 29 can induce antitumor

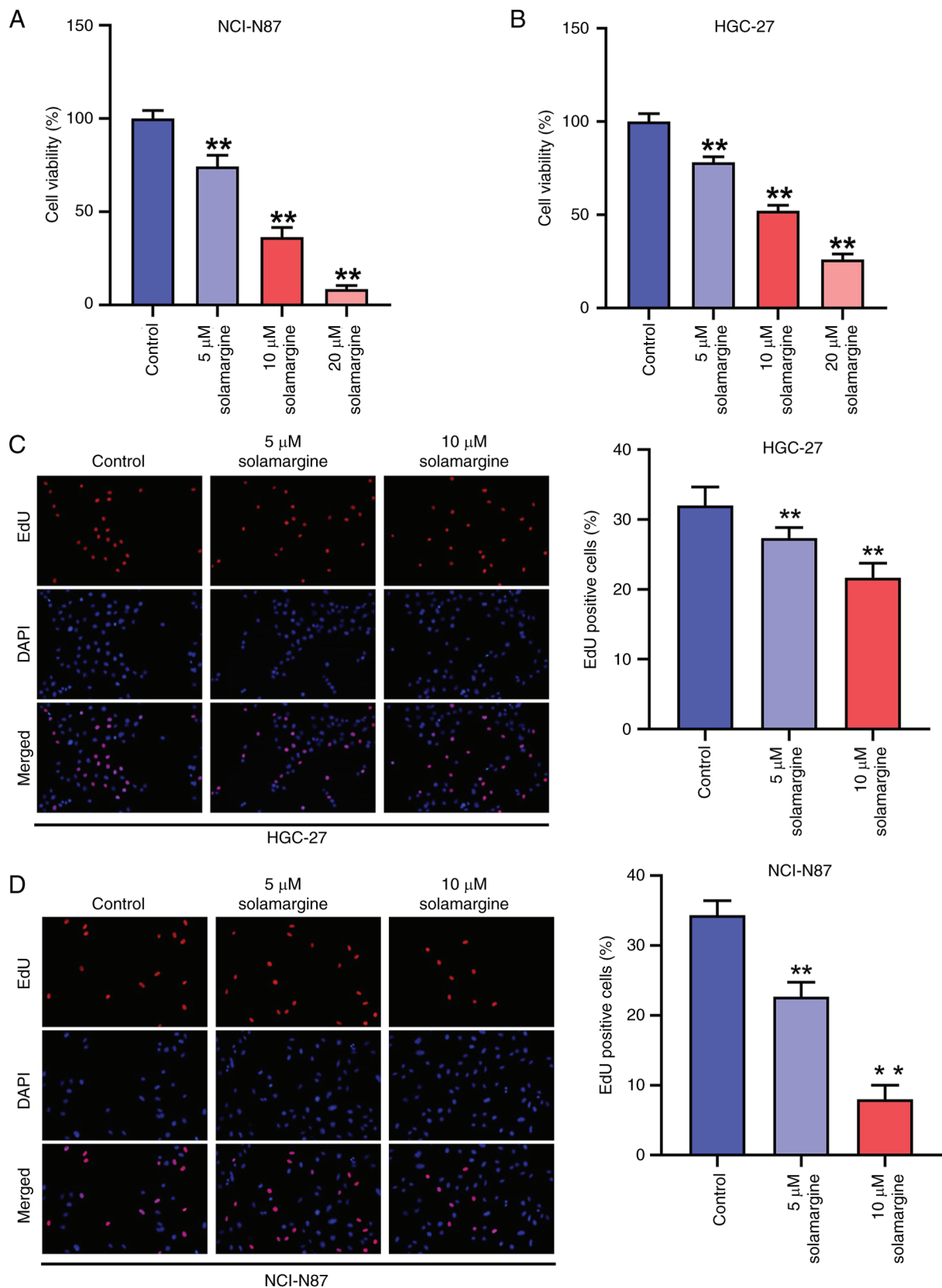


Figure 1. Solamargine significantly reduces the viability and proliferation of GC cells. GC cells were treated with 5, 10 or 20 μ M solamargine for 48 h. The viability of (A) NCI-N87 and (B) HGC-27 cells was assessed using Cell Counting Kit-8 assays. The proliferation of (C) HGC-27 and (D) NCI-N87 cells was investigated using EdU staining. Magnification, x200. ** P <0.01 vs. Control. GC, gastric cancer; EdU, 5-ethynyl-2'-deoxyuridine.

immunity by downregulating STAT3 to inhibit the expression levels of PD-L1 in GC. Additionally, Wang *et al* (30)

revealed that pumiliol can increase the NPM3/NPM1 axis to promote PD-L1-mediated immune escape in GC. These

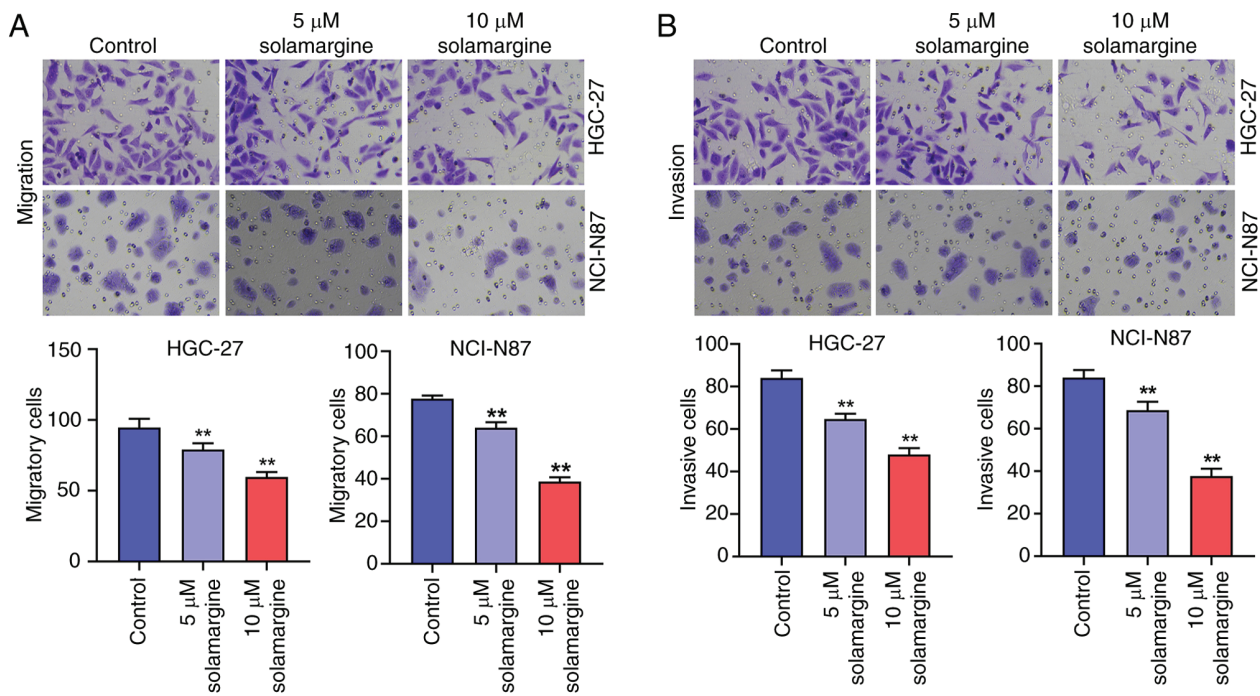


Figure 2. Solamargine significantly reduces the migration and invasion of gastric cancer cells. (A) Migration and (B) invasion of NCI-N87 and HGC-27 cells were investigated using Transwell assays. Magnification, x200. **P<0.01 vs. Control.

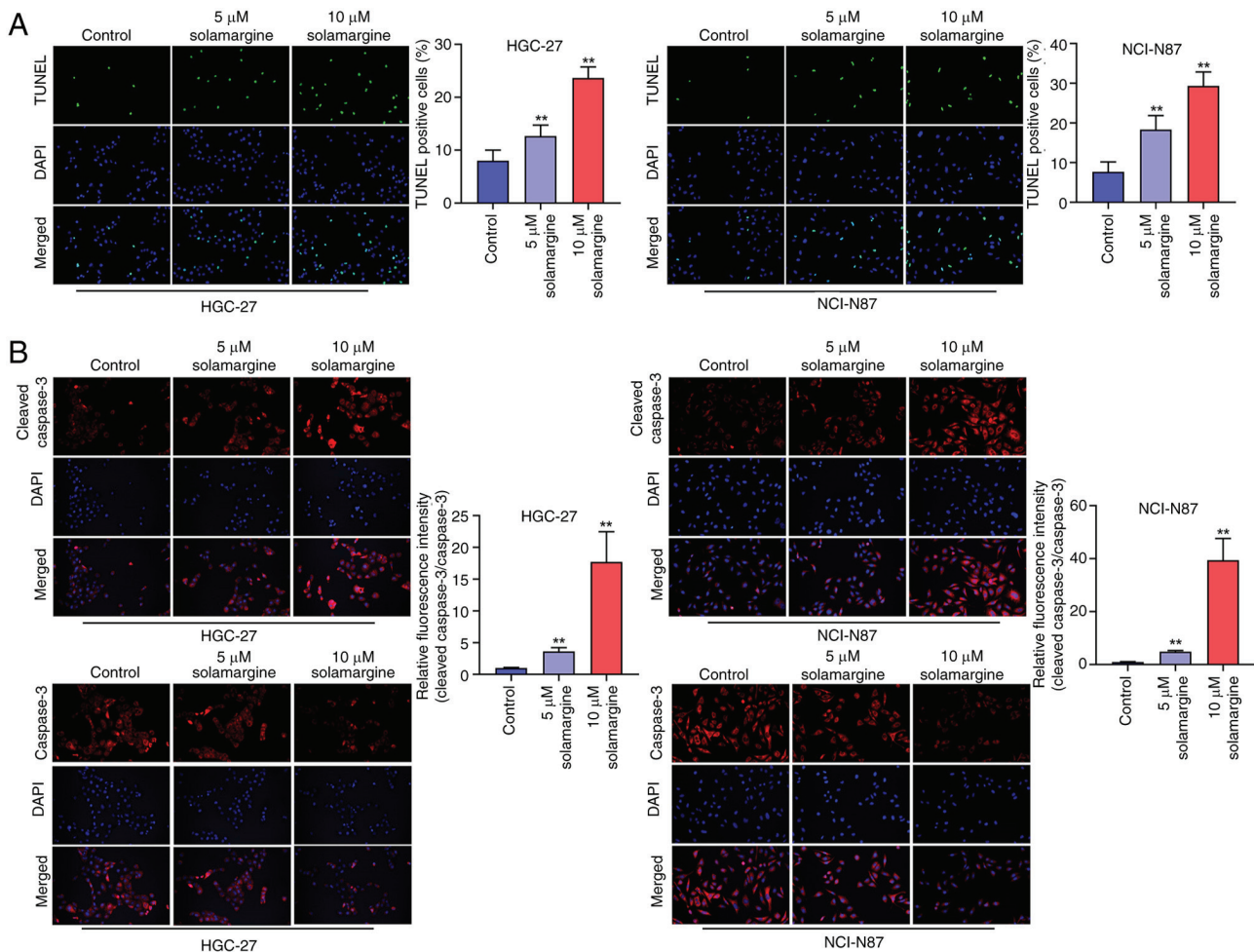


Figure 3. Solamargine significantly increases apoptosis in GC cells through the caspase 3 pathway. (A) Apoptosis of GC cells was assessed using TUNEL staining. (B) Protein expression levels of cleaved caspase 3 were assessed using immunofluorescence staining. Cleaved caspase 3 expression was normalized to that of caspase 3. Magnification, x200. **P<0.01 vs. Control. GC, gastric cancer.

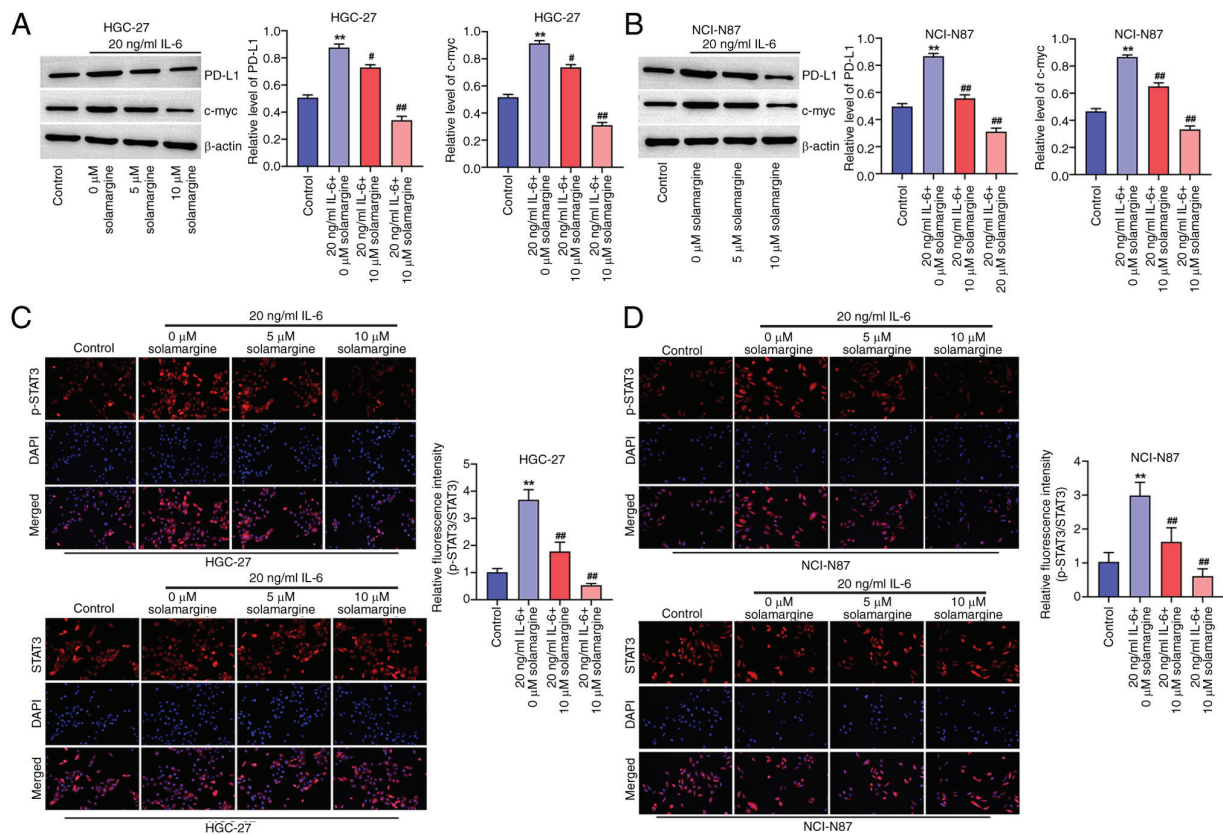


Figure 4. Solamargine reverses the IL-6-induced activation of STAT3/PD-L1 signaling. GC cells were pretreated with 20 ng/ml IL-6 for 24 h, before being co-cultured with Jurkat-T cells for 48 h. Subsequently, GC cells were collected for further analysis. The protein expression levels of c-Myc and PD-L1 in (A) HGC-27 and (B) NCI-N87 cells were assessed using western blotting. Protein levels of p-STAT3 (normalized to STAT3) in (C) HGC-27 and (D) NCI-N87 cells were investigated using immunofluorescence staining. Magnification, x200. ** $P < 0.01$ vs. Control. # $P < 0.05$ and ## $P < 0.01$ vs. IL-6 alone. p-, phosphorylated; PD-L1, programmed cell death ligand 1; GC, gastric cancer.

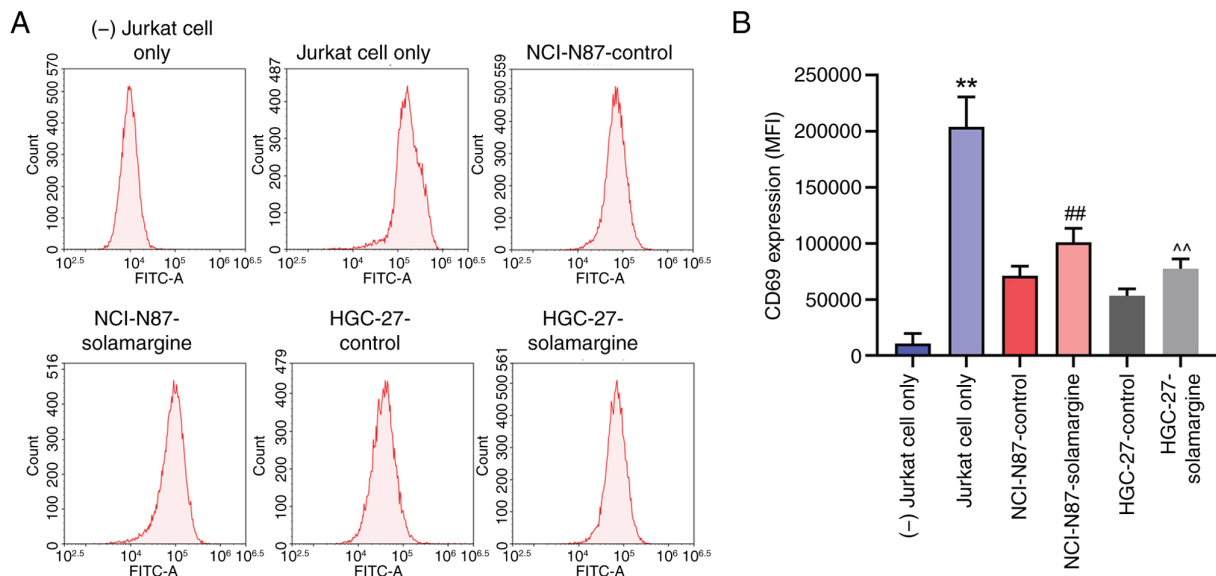


Figure 5. Solamargine activation of T cells. Jurkat T cells were activated using stimulation with anti-CD3/CD28 antibodies and then co-cultured with non-treated or 10 μM solamargine pretreated NCI-N87 or HGC-27 cells. Subsequently, the Jurkat T cells were collected. (A) Representative flow cytometry histograms and (B) the MFI of CD69 in Jurkat T cells assessed using flow cytometry. ** $P < 0.01$ vs. (-) Jurkat T cell only. ## $P < 0.01$ vs. NCI-N87 control. ^^ $P < 0.01$ vs. HGC-27 control. MFI, mean fluorescence intensity. (-) Jurkat T cell indicates Jurkat T cell without CD3/CD28 stimulation.

aforementioned findings suggest that solamargine may increase the antitumor immunity during the progression of GC by inhibiting STAT3/PD-L1 signaling.

However, the present study has a number of limitations. The mechanisms underlying the effect of solamargine on GC requires further investigation. Additionally, *in vivo* studies are

required to verify the results of the present study. In addition, solamargine in combination with other therapies including chemotherapy or targeted therapy should be investigated in future.

In summary, the present study indicated that solamargine can inhibit GC cell proliferation and invasion by inactivating the STAT3 and PD-L1 signaling pathways. This finding may provide a novel theoretical basis for drug discovery for the treatment of GC.

Acknowledgements

Not applicable.

Funding

The present study was supported by the Xiangtan Science and Technology Bureau Project (Clinical study of endoscopic submucosal dissection in the treatment of early carcinoma and precancerous lesions of the digestive tract; grant no. SF-YB20171007).

Availability of data and materials

The data generated in the present study may be requested from the corresponding author.

Authors' contributions

XL and LS designed the study. WL, BL and LL performed the experiments. XL and YS analyzed the data. WL and YS prepared the manuscript. All authors read and approved the final version of the manuscript and XL and LS confirm the authenticity of all the raw data.

Ethics approval and consent to participate

Not applicable.

Patient consent for publication

Not applicable.

Competing interests

The authors declare that they have no competing interests.

References

- Jeon M, Jang H, Jeon H, Park CG and Kim S: Long-term late effects in older gastric cancer survivors: Survival analysis using Cox hazard regression model by retrospective electronic health records. *Support Care Cancer* 32: 29, 2023.
- Sun Z, Liu Y, Deng H, Wang S, Zhang J, Xing C and Xu C: Modified Chaishao Liujunzi Decoction inhibits bile acid-induced gastric intestinal metaplasia: From network prediction to experimental verification. *Aging (Albany NY)* 15: 13998-14018, 2023.
- Fang S, Liu Z, Qiu Q, Tang Z, Yang Y, Kuang Z, Du X, Xiao S, Liu Y, Luo Y, *et al*: Diagnosing and grading gastric atrophy and intestinal metaplasia using semi-supervised deep learning on pathological images: Development and validation study. *Gastric Cancer* 27: 343-354, 2024.
- Zhu Y, Huang C, Zhang C, Zhou Y, Zhao E, Zhang Y, Pan X, Huang H, Liao W and Wang X: LncRNA MIR200CHG inhibits EMT in gastric cancer by stabilizing miR-200c from target-directed miRNA degradation. *Nat Commun* 14: 8141, 2023.
- Pei H, Yang J, Li W, Luo X, Xu Y, Sun X, Chen Q, Zhao Q, Hou L, Tan G and Ji D: *Solanum nigrum* Linn: Advances in anti-cancer activity and mechanism in digestive system tumors. *Med Oncol* 40: 311, 2023.
- Long K, Zhou H, Li Y, Liu L and Cai J: The value of chest computed tomography in evaluating lung cancer in a lobe affected by stable pulmonary tuberculosis in middle-aged and elderly patients: A preliminary study. *Front Oncol* 12: 868107, 2022.
- Han Y, Shi J, Xu Z, Zhang Y, Cao X, Yu J, Li J and Xu S: Identification of solamargine as a cisplatin sensitizer through phenotypical screening in cisplatin-resistant NSCLC organoids. *Front Pharmacol* 13: 802168, 2022.
- Qu X, Xie J, Zhang Y and Wang Z: Solamargine alleviates proliferation and metastasis of cervical cancer cells by blocking the CXCL3-Mediated Erk signaling pathway. *Evid Based Complement Alternat Med* 2022: 7634754, 2022.
- Ge J, Wang P, Ma H and Zhang J: Solamargine inhibits prostate cancer cell growth and enhances the therapeutic efficacy of docetaxel via Akt Signaling. *J Oncol* 2022: 9055954, 2022.
- Huang S, Sun M, Ren Y, Luo T, Wang X, Weng G and Cen D: Solamargine induces apoptosis of human renal carcinoma cells via downregulating phosphorylated STAT3 expression. *Oncol Lett* 26: 493, 2023.
- Cha JH, Chan LC, Li CW, Hsu JL and Hung MC: Mechanisms Controlling PD-L1 expression in cancer. *Mol Cell* 76: 359-370, 2019.
- Ai L, Xu A and Xu J: Roles of PD-1/PD-L1 Pathway: Signaling, cancer, and beyond. *Adv Exp Med Biol* 1248: 33-59, 2020.
- Civriz AH, Teke K, Akdas EM, Dillioglugil O, Vural C and Yaprak Bayrak B: The prognostic value of expressions of STAT3, PD-L1, and PD-L2 in Ta/T1 urothelial carcinoma before and after BCG treatment. *Ural Oncol* 41: 486.e1-486.e13, 2023.
- Wen J, Peng H, Wang D, Wen ZM, Liu YT, Qu J, Cui HX, Wang YY, DU YL, Wang T, *et al*: Lipopolysaccharides protect mesenchymal stem cell against cardiac ischemia-reperfusion injury by HMGB1/STAT3 signaling. *J Geriatr Cardiol* 20: 801-812, 2023.
- Erllichman N, Meshel T, Baram T, Abu Raiya A, Horvitz T, Ben-Yaakov H and Ben-Baruch A: The Cell-Autonomous Pro-Metastatic Activities of PD-L1 in Breast Cancer Are Regulated by N-Linked Glycosylation-Dependent Activation of STAT3 and STAT1. *Cells* 12: 2338, 2023.
- Wang R, Ye H, Yang B, Ao M, Yu X, Wu Y, Xi M and Hou M: m6A-modified circNFIX promotes ovarian cancer progression and immune escape via activating IL-6R/JAK1/STAT3 signaling by sponging miR-647. *Int Immunopharmacol* 124(Pt A): 110879, 2023.
- Ye H, Yu W, Li Y, Bao X, Ni Y, Chen X, Sun Y, Chen A, Zhou W and Li J: AIM2 fosters lung adenocarcinoma immune escape by modulating PD-L1 expression in tumor-associated macrophages via JAK/STAT3. *Hum Vaccin Immunother* 19: 2269790, 2023.
- de Carvalho T, Lara P, Jorquera-Cordero C, Aragão CFS, de Santana Oliveira A, Garcia VB, de Paiva Souza SV, Schomann T, Soares LAL, da Matta Guedes PM and de Araújo Júnior RF: Inhibition of murine colorectal cancer metastasis by targeting M2-TAM through STAT3/NF-kB/AKT signaling using macrophage 1-derived extracellular vesicles loaded with oxaliplatin, retinoic acid, and Libidibia ferrea. *Biomed Pharmacother* 168: 115663, 2023.
- Han Y, Liu D and Li L: PD-1/PD-L1 pathway: Current researches in cancer. *Am J Cancer Res* 10: 727-742, 2020.
- Dermani FK, Samadi P, Rahmani G, Kohlan AK and Najafi R: PD-1/PD-L1 immune checkpoint: Potential target for cancer therapy. *J Cell Physiol* 234: 1313-1325, 2019.
- Fan J, Fan F, He J and Sun Y: Agaricus blazei Murill extract FA-2-b- β inhibits gastric cancer cell proliferation by apoptosis by the mitochondrial pathway and blocking the cell cycle. *Asian J Surg* 47: 1560-1561, 2023.
- Han EK, Woo JW, Suh KJ, Kim SH, Kim JH and Park SY: PD-L1 (SP142) expression in primary and recurrent/metastatic triple-negative breast cancers and its clinicopathological significance. *Cancer Res Treat* 56: 557-566, 2023.

23. Anderson HG, Takacs GP, Harris DC, Kuang Y, Harrison JK and Stepien TL: Global stability and parameter analysis reinforce therapeutic targets of PD-L1-PD-1 and MDSCs for glioblastoma. *J Math Biol* 88: 10, 2023.
24. Yu P, Wei H, Li K, Zhu S, Li J, Chen C, Zhang D, Li Y, Zhu L, Yi X, *et al*: The traditional chinese medicine monomer Ailanthone improves the therapeutic efficacy of anti-PD-L1 in melanoma cells by targeting c-Jun. *J Exp Clin Cancer Res* 41: 346, 2022.
25. Liu Y, Liu X, Zhang N, Yin M, Dong J, Zeng Q, Mao G, Song D, Liu L and Deng H: Berberine diminishes cancer cell PD-L1 expression and facilitates antitumor immunity inhibiting the deubiquitination activity of CSN5. *Acta Pharm Sin B* 10: 2299-2312, 2020.
26. Wang J, He X, Jia Z, Yan A, Xiao K, Liu S, Hou M, Long Y and Ding X: Shenqi Fuzheng injection restores the sensitivity to gefitinib in non-small cell lung cancer by inhibiting the IL-22/STAT3/AKT pathway. *Pharm Biol* 62: 33-41, 2024.
27. Li XH, Huang GZ, Xu ZL, Zhao CY, Dong XY, Cui BK and Lin XJ: IL20RB signaling enhances stemness and chemotherapy resistance in pancreatic cancer. *J Transl Med* 21: 911, 2023.
28. Liu C, Shen A, Song J, Cheng L, Zhang M, Wang Y and Liu X: LncRNA-CCAT5-mediated crosstalk between Wnt/ β -Catenin and STAT3 signaling suggests novel therapeutic approaches for metastatic gastric cancer with high Wnt activity. *Cancer Commun (Lond)* 44: 76-100, 2024.
29. Jiang T, Xia Y, Li Y, Lu C, Lin J, Shen Y, Lv J, Xie L, Gu C, Xu Z and Wang L: TRIM29 promotes antitumor immunity through enhancing IGF2BP1 ubiquitination and subsequent PD-L1 downregulation in gastric cancer. *Cancer Lett* 581: 216510, 2024.
30. Wang H, Zhou Z, Zhang J, Hao T, Wang P, Wu P, Su R, Yang H, Deng G, Chen S, *et al*: Pumiliol regulates NPM3/NPM1 axis to promote PD-L1-mediated immune escape in gastric cancer. *Cancer Lett* 581: 216498, 2024.



Copyright © 2024 Liu et al. This work is licensed under a Creative Commons Attribution-NonCommercial-NoDerivatives 4.0 International (CC BY-NC-ND 4.0) License.